

# Cognition-Supervised Saliency Detection: Contrasting EEG Signals and Visual Stimuli

Anonymous Authors

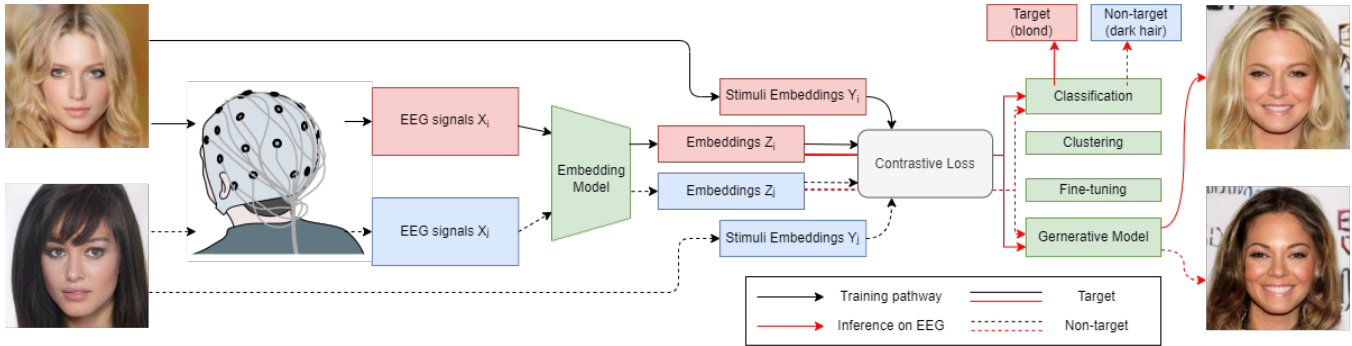


Figure 1: Illustration of cognition-supervised visual saliency detection and its applications in downstream tasks. EEG responses to visual stimuli are used to train embedding models through CLIP loss by contrasting EEG with stimuli image representations. The learned EEG embeddings are applied in downstream tasks such as clustering, classification, fine-tuning personalized models, and conditioning generative models. No manual annotation is needed during training or inference.

## ABSTRACT

Understanding human assessment of semantically salient parts of multimedia content is crucial for developing human-centric applications, such as annotation tools, search and recommender systems, and systems able to generate new media matching human interests. However, the challenge of acquiring suitable supervision signals to detect semantic saliency without extensive manual annotation remains significant. Here, we explore a novel method that utilizes signals measured directly from human cognition via electroencephalogram (EEG) in response to natural visual perception. These signals are used for supervising representation learning to capture semantic saliency. Through a contrastive learning framework, our method aligns EEG data with visual stimuli, capturing human cognitive responses without the need for any manual annotation. Our approach demonstrates that the learned representations closely align with human-centric notions of visual saliency and achieve competitive performance in several downstream tasks, such as image classification and generation. As a contribution, we introduce an open EEG/image dataset from 30 participants, to facilitate further research in utilizing cognitive signals for multimodal data analysis, studying perception, and developing models for cross-modal representation learning.

## CCS CONCEPTS

• Human-centered computing → HCI design and evaluation methods; • Computing methodologies → Cognitive science.

## KEYWORDS

Electroencephalography, EEG, Contrastive Learning, Generative Modeling, Neuroimaging

## 1 INTRODUCTION

Human cognition excels at detecting salient information from various media, rapidly identifying what is important for an individual in a specific context or multimedia experience. This innate ability to discern salient parts of stimuli is crucial for a range of multimedia applications, including generating personalized content recommendations, interfaces, and multimedia experiences. However, replicating this capability in machines, particularly in a way that reflects an individual's perception of semantic saliency, remains a significant challenge. Traditional machine learning approaches often rely on large datasets of implicitly obtained signals, such as click data [27, 37, 50] or dwell time [59], from platforms that expose information to their users, such as social media or video streaming services. These data, often combined with visual information under a supervised learning framework [58], serve as proxies for cognitive responses to salient features. However, these supervision data may not always capture the nuanced cognitive preferences of individuals and is dependent on availability of behavioral data, such as clicks.

In this work, we propose an alternative approach, *cognition-supervised saliency detection*, to capture human cognitive responses to visual information without reliance on manual labels or behavioral data. Our method utilizes natural human cognitive reactions evoked by visual perception of media content and measured via

Unpublished working draft. Not for distribution.

Permission to make digital or hard copies of all or part of this work for personal or professional use, is granted by ACM, provided that the copies are distributed for profit or commercial advantage and that copies bear this notice and the full citation on the first page. Copyrights for components of this work owned by others than the author(s) must be honored. Abstracting with credit is permitted. To copy otherwise, or to publish, to post on servers or to redistribute to lists, requires prior specific permission and/or a fee. Request permissions from [permissions@acm.org](mailto:permissions@acm.org).

ACM MM, 2024, Melbourne, Australia

© 2024 Copyright held by the owner/author(s). Publication rights licensed to ACM.

ACM ISBN 978-x-xxxx-xxxx-x/YY/MM

<https://doi.org/10.1145/nnnnnnn.nnnnnn>

117 electroencephalogram (EEG). Specifically, participants are exposed  
118 to visual information while their EEG signals evoked in response  
119 to perception are recorded. These EEG data are then employed in  
120 a self-supervision framework to learn representations of salient  
121 semantic visual features eliciting variations in cognitive responses.

122 Integrating brain responses into machine learning has historically  
123 been challenging. Prior research on visual saliency detection  
124 leveraging brain responses often depended on manually labeled  
125 data [12, 44, 62] or the fine-tuning of models pretrained on such  
126 data [14, 18, 48, 53]. Unsupervised methods, conversely, tend to  
127 underperform with brain data due to its inherent noise and com-  
128 plexity [40]. In scenarios such as supervised binary classification  
129 using only single-trial data with complex visual stimuli, accuracy  
130 typically remains modest – for instance, 0.78 for differentiating  
131 human faces from objects [33], about 0.7 for within-subject and  
132 roughly 0.4 for cross-subject comparisons [33, 63], 0.708 for Ima-  
133 geNet subsets [2], and under 0.6 for text stimuli [19]. Moreover,  
134 certain earlier studies addressing similar challenges have been crit-  
135 icized for relying on confounded datasets [34]. As a result, using  
136 brain signals as a direct source of supervision for machine learning  
137 models is facing two fundamental problems: achieving a performance  
138 that has utility for practical applications and learning without manu-  
139 ally labeled data.

140 Our approach tackled both of these problems. It learns repre-  
141 sentations of semantic visual saliency as perceived by the brain,  
142 utilizing unlabeled EEG data contrasted with visual stimuli for su-  
143 pervision. The model is crafted to differentiate between target and  
144 non-target saliency, based on participants’ brain responses.

145 Utilizing this model, we explore two primary research questions:

146 **RQ1:** Can representations of semantic saliency be directly learned  
147 from EEG data as a supervision signal?

148 **RQ2:** Do the learned representations accurately capture the salient  
149 features in downstream tasks?

150  
151 With our experiment results, we demonstrated that the learned  
152 representations reflect the desired semantic visual saliency better  
153 than any single modality representations, and linear classifiers built  
154 on top of them have performance comparable to supervised models.  
155 We also tested our method in personalization scenarios where a  
156 base model can flexibly adapt to a small amount of personal data.  
157 In a generative downstream task, the learned representations are  
158 used to successfully condition the generated images to fully match  
159 the semantic saliency given in the task.

160 Additionally, to further research in this area, we are releas-  
161 ing an open, anonymized EEG dataset from 30 participants. This  
162 dataset, designed with specific semantic saliency detection tasks for  
163 multimedia content, aims to promote advancements in cognition-  
164 supervised models.

165 In summary, our main contributions are:

- 166 • Introducing a novel approach for contrastively training mod-  
167 els with cognitive EEG responses to visual multimedia stim-  
168 uli, to learn representations of semantic visual saliency.
- 169 • Releasing a new open and anonymized EEG dataset from  
170 30 participants, complete with a comprehensive codebase,  
171 to encourage research in cognition-supervised models for  
172 multimedia applications.

## 2 RELATED WORK

175  
176 In recent years, the integration of brain signals with machine learn-  
177 ing has garnered considerable attention for its potential to enhance  
178 both the performance and interpretability of models. Among the  
179 array of brain-computer interface devices, electroencephalogra-  
180 phy (EEG) signals stand out as a favored modality, offering rich,  
181 albeit noisy, data for supervised machine learning models. EEG is  
182 valued for its non-intrusive nature, high temporal resolution, and  
183 cost-effectiveness.

184 However, EEG signals are inherently challenged by limited spa-  
185 tial resolution and susceptibility to artifacts and noise from subject  
186 movements, which can significantly impede the efficacy of EEG-  
187 based machine learning models. This is particularly prominent for  
188 models addressing cognitive processes like visual semantic saliency  
189 recognition in real-world media content. The modest spatial resolu-  
190 tion of EEG complicates the accurate localization of neural activity  
191 tied to visual cognition, and noise can further obscure the cognitive  
192 signals of interest.

193 Decoding EEG signals has enabled a wide range of applications,  
194 including emotion recognition [3, 24] for affective multimedia ex-  
195 periences, mental workload assessment [4, 46] for adaptive user  
196 interfaces, and multimedia content understanding [29, 42]. These  
197 applications are grounded in supervised EEG classification mod-  
198 els, which facilitate the effective use of brain data across various  
199 contexts.

200 However, traditional supervised machine learning approaches  
201 rely on manual annotations, presenting challenges related to cost  
202 of training the models and subjectivity of the training data. Manual  
203 annotations, requiring domain experts to label vast quantities of  
204 multimedia data, are both time-consuming and resource-intensive.  
205 Moreover, the subjectivity inherent in human annotations can lead  
206 to inter-annotator variability, undermining the reliability and con-  
207 sistency of annotations, especially for subjective phenomena like  
208 emotions and cognitive responses to multimedia content. This may  
209 force "one-size-fits-all" models and ignore the need for personalized  
210 models of human cognition.

211 To address these limitations, there is a growing need for un-  
212 supervised and self-supervised approaches that leverage EEG as  
213 supervisory signals to train machine learning models. Recent re-  
214 search has explored the direct use of brain signals as supervisory  
215 signals for machine learning models [8, 9, 16, 32]. Self-supervised  
216 learning with EEG data may provide potentially more objective  
217 and quantifiable measures of brain activity, leading to more reliable  
218 and cost-effective annotations compared to traditional methods  
219 requiring expert knowledge for manual annotation. Moreover, the  
220 real-time capture of brain responses enhances the adaptability and  
221 robustness of machine learning models, allowing them to dynam-  
222 ically respond to changes in brain states during perception of digital  
223 information.

224 A series of earlier studies on EEG-based image reconstruction suf-  
225 fer from confounded EEG data due to specific experimental block de-  
226 signs. This includes the EEG-GAN approach [43, 52], Thoughtviz [54],  
227 Brain2Image [29], EEG-ChannelNet [42], and numerous subse-  
228 quent research on the same datasets such as EEG2IMAGE [51],  
229 DM-RE2I [61], NeuroGAN [38], and GDN-GAN [30]. To this end,  
230 subsequent analyses [1, 2, 34] have identified a critical flaw in these  
231

175  
176  
177  
178  
179  
180  
181  
182  
183  
184  
185  
186  
187  
188  
189  
190  
191  
192  
193  
194  
195  
196  
197  
198  
199  
200  
201  
202  
203  
204  
205  
206  
207  
208  
209  
210  
211  
212  
213  
214  
215  
216  
217  
218  
219  
220  
221  
222  
223  
224  
225  
226  
227  
228  
229  
230  
231  
232

approaches: the block design in data collection introduces temporal correlations between the presentation order of stimulus class and the experiment duration. Attempts to replicate these studies have suggested that models were learning to recognize the order of stimuli presentation rather than the genuine cognitive reactions to the stimuli [34].

In parallel, contrastive learning methods have gained significant attention in the broader field of machine learning [10, 20–22, 45, 56, 57]. Contrastive learning aims to develop robust and meaningful representations without explicit annotations, by maximizing the similarity between positive pairs (similar samples) and minimizing it between negative pairs (dissimilar samples). The efficacy of contrastive learning has been proven in areas like large language models [45], image embeddings [25], and audio data [47], yet its application in EEG-based machine learning to be paired with multimedia data is still relatively unexplored. Similar contrastive methods have been applied to EEG data for tasks such as sleep stage classification [26], emotion recognition [39], and pathology screening [6]. These methods often rely on carefully designed data augmentation or combinations of transformations. However, identifying effective data augmentation techniques for EEG data in multimedia scenarios remains a challenge. A recent study [26] highlighted how improper transformation choices could significantly reduce test accuracy, from 82.90% to 48.15%.

Moreover, focusing contrastive learning on a single modality may overlook valuable information from other modalities, especially in multimedia applications that typically involve multiple modalities. This challenge was tackled by supervised contrastive learning [20], which enhances image pair augmentation with labeling for better grouping. Another study [57] introduced a hierarchical semantic alignment strategy to assess the semantic similarity between images. Additionally, a multimodal contrastive training method [60] employed multiple loss functions to leverage the intrinsic data structure of each modality.

Our work is inspired by the well-known language supervision approach CLIP [45], which learns representations from paired text and image data to align across two modalities. Similarly, our embedding model aligns representations from paired EEG and visual stimuli data, effortlessly obtained from data collection in multimedia scenarios. Unlike merely decoding EEG signals to categorical or simplistic stimuli, our contrastive approach bridges EEG with high-dimensional multimedia stimuli. In a manner akin to CLIP, which is grounded in natural language supervision, we define our method as cognition-supervised learning.

A recent study [49] investigated non-linear techniques to learn a consistent latent space of joint behavior and neural data across subjects, applying this method to various animal datasets. However, it's crucial to recognize that this data was acquired through intrusive methods, using implanted electrodes or probes, which are more challenging to apply to human subjects in multimedia contexts than non-intrusive EEG signals. This study aimed at movie frame reconstruction, focusing on the sequence of movie frames rather than their content, which restricts its applicability to multimedia applications featuring diverse and dynamic content.

Consequently, a significant research opportunity exists for effective cognition-supervised learning within multimedia applications. To fill this gap, we introduce a novel approach that leverages the

contrast between EEG data and multimedia stimuli as a supervisory signal. Our method benefits from label-free learning using EEG data and integrates stimuli information to remain effective even with a limited amount of EEG data, which might be insufficient for self-supervision if relying solely on EEG signals.

## 3 METHODS

### 3.1 Data Collection and Preparation

To explore the feasibility of cognition-supervised learning, we conducted neurophysiological experiments to gather EEG responses to generated visual stimuli. The acquisition of neurophysiological data and subsequent experiments received approval from the ethical review board of social and behavioral sciences at *anonymous organization*, adhering to the Declaration of Helsinki<sup>1</sup>. Informed consent was signed by each participant to acknowledge their rights. Participants were compensated with vouchers for the local cinema.

**Visual Stimuli Preparation.** We selected generated images of faces as visual stimuli, recognizing that humans exhibit strong responses to facial stimuli [55]. Generated images were chosen over real ones to control for variances in semantics and confounding visual features, thereby minimizing brain responses related to recognition effects. This approach ensures a homogeneous dataset that facilitates strict semantic-level evaluation in generative tasks. A random sample of 70,000 images was generated using a progressive GAN<sup>2</sup> [28], pre-trained on the CelebA dataset [35]. The raw images, with a resolution of 1024 by 1024 pixels, were manually screened by researchers to remove images with visual artifacts, such as distorted faces or evident signs of artificiality, to ensure brain responses reflected semantic saliency rather than artifact recognition. These images were categorized into eight groups based on semantic saliency: smiling, not smiling, female, male, young, old, dark hair, and light hair (blond).

**Participants.** Neurophysiological data were collected from thirty participants (self-reported 13 female and 17 male, mean age 28 years (SD = 7.14, Min = 18, Max = 45)) at *anonymous organization*. Participants were healthy with normal or corrected-to-normal vision.

**Apparatus, Tasks, and Procedure** Participants were exposed to eight recognition tasks sequentially, each corresponding to one of the semantic saliency groups (e.g., female, smiling). An elliptic grey frame was used to obscure the backgrounds of all images. EEG data were captured using 32 Ag/AgCl electrodes, placed according to the 10–20 system, and connected to a QuickAmp USB (BrainProducts GmbH, Gilching, Germany) amplifier with a sampling rate of 2,000 Hz. Eye movements were monitored for artifact removal through two pairs of bipolar electrodes positioned near the eyes (1 cm lateral to the left and right canthi, and 2 cm above and below the right pupil).

For each task, stimuli were labeled binary according to their semantic saliency. For instance, in the "smile" task, participants viewed images of smiling (target) and non-smiling (non-target) faces. Participants were asked to mentally note images matching

<sup>1</sup><http://www.wma.net/en/20activities/10ethics/10helsinki/>

<sup>2</sup>[https://github.com/tkarras/progressive\\_growing\\_of\\_gans](https://github.com/tkarras/progressive_growing_of_gans) under the attribution-noncommercial 4.0 international (cc by-nc 4.0) license

the task description without any physical response. Each task iteration presented twenty target and twenty non-target images in a random sequence. Stimuli were displayed using a rapid serial visual presentation (RSVP) method at a 500 ms interval. A demonstration task was conducted before each main task to confirm participants' understanding, where they were to identify images featuring the specified semantic attribute.

**Data Preprocessing.** Post data collection, we applied standard signal cleaning techniques [36] to enhance the signal-to-noise ratio, involving only automatic methods that do not necessitate any additional labeled data. This included applying a band-pass filter within the 0.2–35 Hz frequency range and time-locking epochs from -200 to 900 ms relative to stimulus onset, with baseline correction using the pre-stimulus interval from -200 to 0 ms. Eyeblick artifacts were eliminated using a threshold heuristic, setting the threshold to the 200th largest mean absolute value across epochs and channels, within a [10,80] range. After preprocessing and balancing, an average of 1144 epochs per participant remained. Data aggregated across participants revealed a typical P300 effect, with increased potentials for target stimuli observable from 250 ms post-stimulus onset until 600 ms, as shown in Figure 2. This result validates the anticipated ERP effect on a population average through our experimental setup.

### 3.2 Cognitive Supervision

Cognition-supervised learning is predicated on the fundamental observation that the human brain differentially responds to perceptual stimuli. This principle implies that the contrast between visual stimuli and brain responses can act as a supervision signal, enabling direct learning from preferences reflected in cognitive processes. This contrastive learning framework allows for the development of a loss function that relies solely on EEG data and stimuli, obviating the need for manual annotations.

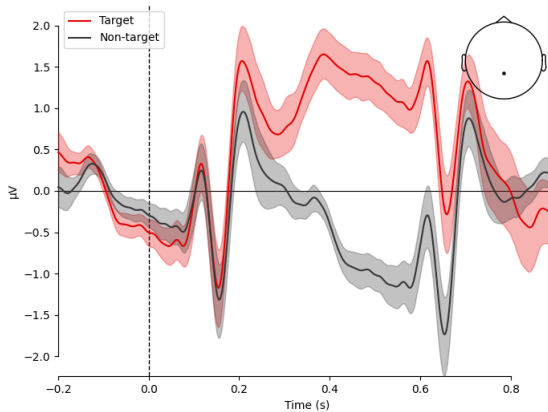


**Figure 2: Average event-related potentials (ERPs) across participants at the Pz electrode for target and non-target stimuli, illustrating a P300 effect.**

To facilitate cognition-supervised learning, we introduce a model that embeds EEG signals. For each stimulus image generated from a latent vector  $Y \in \mathbb{R}^L$  (where  $L$  is the dimension), we represent the corresponding epoched EEG response as  $X \in \mathbb{R}^{C \times T}$ , with  $C$  denoting the number of channels and  $T$  the number of time steps in the epoch.

Initially, we considered employing a regression model  $f_{reg} : \mathbb{R}^{C \times T} \rightarrow \mathbb{R}^L$  to reconstruct the stimulus vector from EEG inputs. However, this approach tended to overfit to noise and showed limited generalizability. Moreover, reconstructing the entire stimulus vector from EEG is impractical since only salient semantic features and major facial attributes are discernible to participants. Consequently, we adopted a noise contrastive estimation using a CLIP loss [45], aiming to embed semantic saliency as perceived by participants.

Our proposed embedding model  $f_{\text{embed}} : \mathbb{R}^{C \times T} \rightarrow \mathbb{R}^L$  is trained with an EEG signal  $X$  and its associated stimulus vector  $Y$ , alongside a set of negative stimulus vectors  $Y_i$  for  $i \in \{2, 3, \dots, N\}$ , ensuring  $Y_i$  differ from  $Y$ . The negative set is sampled from the remaining stimuli vectors in the dataset while avoiding duplication of  $Y$  and  $Y_i$ .  $Y_1 := Y$  is treated as the positive sample.

The model  $f_{\text{embed}}$  predicts the probability  $\hat{p}_j = \mathbb{P}[Y_j = Y]$  by calculating the dot product between  $Z := f_{\text{embed}}(X)$  and each  $Y_j$ , followed by a Softmax function. The probability is defined as:

$$\hat{p}_j = \frac{e^{\langle Z, Y_j \rangle}}{\sum_{j'=1}^N e^{\langle Z, Y_{j'} \rangle}} \quad (1)$$

where  $\langle \cdot, \cdot \rangle$  indicates the inner product.

$f_{\text{embed}}$  is optimized using cross-entropy between the actual probability  $p_j$  and the estimated  $\hat{p}_j$ , where  $p_j = 1$  iff  $j = 1$ , and  $p_j = 0$  otherwise. The loss function simplifies to:

$$L_{\text{CLIP}}(p, \hat{p}) = -\langle Z, Y \rangle + \log\left(\sum_{j=2}^N e^{\langle Z, Y_j \rangle}\right) \quad (2)$$

### 3.3 Model Structure

To accommodate inter-subject variability while capturing the intrinsic structures of EEG signals, we employ a deep neural network,  $f_{\text{embed}}$ , processing raw, vectorized EEG signals. Additionally, a one-hot encoded vector representing the participant is input to the network, which outputs an embedding vector  $Z$  of the same dimension as the stimulus vector  $Y$ . The network architecture comprises two components: (1) a participant-specific convolution matrix and (2) a series of fully connected layers.

**Fully Connected Layers.** The embedding model features four fully connected layers. The first three layers each have 2048 hidden nodes and utilize a LeakyReLU activation function with  $\alpha = 0.3$ . Following each of these layers is a Dropout layer with a dropout rate of 0.5. The final layer outputs 512 nodes without any activation function.

**Participant-Specific Matrix.** To accommodate variability across participants within a unified model, we implement a strategy similar to that described in [17]. A participant-specific layer, placed at the outset of the network, contains a trainable  $C \times C$  matrix for each participant. This matrix is applied to the vectorized  $C \times T$  EEG

signal across channels, initialized near the identity matrix with slight random perturbations.

**Data Augmentation.** To enhance model generalization and mitigate overfitting, we apply random data augmentation during training. Initially, each EEG vector  $x \in \mathbb{R}^{C \times T}$  is scaled by a random vector  $c \in [0.95, 1.05]^C$ . Subsequently, we perform a random crop and resize on the vector to  $x' \in \mathbb{R}^{C \times T}$ , selecting an interval  $[l, r]$  where  $l \in [0, \frac{T}{10}]$  and  $r \in [T - \frac{T}{10}, T]$ . For the validation set, we consistently crop and resize the data within the fixed interval  $[\frac{T}{20}, T - \frac{T}{20}]$ , excluding the random scaling.

## 4 EXPERIMENTS

In this section, we evaluate the efficacy of cognitive supervision on embedding models through structured experiments. Initially, t-SNE visualization assesses embedding space clustering for target versus non-target saliency. Next, unsupervised clustering examines the embedding space's alignment with target and non-target distinctions. Subsequently, a linear evaluation protocol [5, 13, 15, 23, 31, 41] determines if classifiers on saliency embeddings outperform non-supervised data. We then explore personalized model tuning. Finally, a qualitative assessment is conducted using generative adversarial networks to visualize cognition-supervised predictions.

**Dataset.** Our dataset consists of EEG signal and stimuli vector pairs from 30 participants, comprising a total of 35490 pairs. To ensure that the individual factor is accounted for, we mixed all participant data while retaining a unique participant identifier to apply the participant-specific matrix. For the unsupervised task, we trained and evaluated our embedding model on the entire dataset. For linear classification tasks, we employed 10-fold validation by randomly splitting the dataset into training and testing sets and reported the mean of evaluation metrics. All experiments were repeated three times with different random seeds. To accurately reflect the variability due to methodological randomness rather than distribution differences, results are averaged across the tasks for each run, and standard deviations of these averages are computed and reported alongside all evaluations.

**Hyperparameters and Hardware.** In all experiments, the brain embedding model is trained with Adam optimizers with an initial learning rate  $1e-4$ ,  $\beta_1 = 0.9$ ,  $\beta_2 = 0.999$ , and a weight decay  $1e-4$ . The mini-batch size is set to 256 in all experiments. We conducted all experiments on Tensorflow with a single Nvidia GeForce RTX 3070 Ti GPU. Each embedding model in the unsupervised clustering experiments, linear evaluation experiments and the base model in the personalized experiments are trained with 500 epochs. The personalized model is fine-tuned by 100 iterations by using the base model, with all other parameters frozen except the participant-specific matrix.

### 4.1 t-SNE Visualization of Embeddings

First, we provide an intuitive understanding of the learned embeddings by visualizing the feature space of EEG, stimuli, and embedding space visualized via t-SNE as shown in Figure 3. The data points are colored according to the target and non-target stimuli. The learned embedding space separates the data significantly better than either of the original modalities. The target and non-target

data points are not linearly separable in either the EEG or stimuli space, but they are clearly separable in the learned embedding space.

### 4.2 Unsupervised Clustering and Classification

The discernible patterns within the t-SNE visualizations inspire us to perform unsupervised clustering to automatically distinguish between target and non-target clusters, leveraging the model's innate capability to differentiate salient features without label assistance.

**Evaluation Procedure.** Employing KMeans with  $k = 2$  on the embeddings, we identify two clusters. The one with a higher average P300 effect is designated as the Target cluster ( $C_T$ ), while the other is recognized as the Non-target cluster ( $C_N$ ). This method allows for the autonomous classification of the dataset into meaningful groups that correspond to the stimuli's inherent saliency, without any reliance on explicit labels. We compute the clustering accuracy as the ratio of correctly classified samples to the total number of samples.

**Control Models.** For context, we compare our approach against KMeans clustering applied to (1) stimuli vectors, (2) flattened EEG signals, and (3) their concatenated forms. This comparison highlights the efficacy of our embeddings in capturing cognitive patterns. The highest clustering accuracy over all clusters permutations is reported for control models.

**Results.** Table 1 summarizes the clustering accuracies, underscoring our model's superiority in discerning between target and non-target clusters across various tasks. This outcome confirms the model's effectiveness in capturing participant-perceived salient features purely through unsupervised learning.

### 4.3 Linear Evaluation

**Evaluation procedure.** To evaluate the efficiency of the learned saliency representations, we follow the commonly used linear evaluation protocol, by training a linear classifier on top of the frozen embeddings. The dataset is randomly split into a training set and a testing set with disjoint sets of stimuli. We then train our contrastive embedding model on the training set and then compute the embeddings with frozen model weights. A single-layer binary classifier  $C(\cdot) : \mathbb{R}^{512} \rightarrow \{0, 1\}$  is trained on the embeddings from the training set using the explicit labels of stimuli images. The classifier is then evaluated on the test set using the labels with classification accuracy.

**Control models.** To provide a basis for comparison, we also consider three control models as the baseline. The first is a well-known supervised EEGNet [33] structure to estimate the upper limit of performance for the cognition-supervised models and highlights the difficulties of the task. The second is a linear discriminant analysis model (LDA) [7] to estimate the separability of raw EEG signals. Both control models are trained on the raw EEG signals and the explicit labels. The third baseline model is a randomly permuted cognition-supervised EEG classifier to determine a lower bound performance, in which the pairs of EEG signals and stimuli vectors are shuffled so that the pairs are broken.

**Results.** Table 2 shows the mean accuracies of all models for each task. The linear classifiers on saliency embeddings consistently outperform the random baseline and the LDA models, indicating

465  
466  
467  
468  
469  
470  
471  
472  
473  
474  
475  
476  
477  
478  
479  
480  
481  
482  
483  
484  
485  
486  
487  
488  
489  
490  
491  
492  
493  
494  
495  
496  
497  
498  
499  
500  
501  
502  
503  
504  
505  
506  
507  
508  
509  
510  
511  
512  
513  
514  
515  
516  
517  
518  
519  
520  
521  
522

523  
524  
525  
526  
527  
528  
529  
530  
531  
532  
533  
534  
535  
536  
537  
538  
539  
540  
541  
542  
543  
544  
545  
546  
547  
548  
549  
550  
551  
552  
553  
554  
555  
556  
557  
558  
559  
560  
561  
562  
563  
564  
565  
566  
567  
568  
569  
570  
571  
572  
573  
574  
575  
576  
577  
578  
579  
580

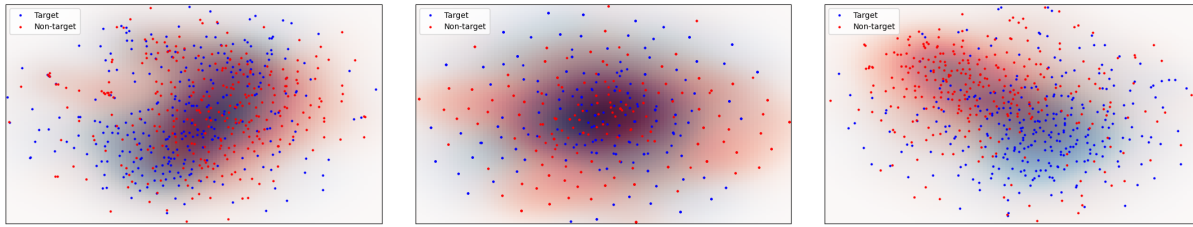


Figure 3: Visualization of feature space of (left) EEG, (middle) stimuli and (right) embedding space visualized via t-SNE. The learned embedding space separates the data significantly better than either of the original modalities.

Table 1: Clustering accuracies on all tasks with different inputs for KMeans.

KMeans input	female	male	blond	darkhaired	smiles	nosmile	old	young	Mean
stimuli vectors	0.57±0.02	0.56±0.06	0.54±0.01	0.53±0.03	0.51±0.01	0.52±0.01	0.52±0.02	0.53±0.01	0.536±0.011
EEG signals	0.57±0.01	0.51±0.01	0.56±0.01	0.52±0.01	0.57±0.01	0.50±0.01	0.52±0.01	0.55±0.01	0.537±0.001
concatenated	0.55±0.02	0.53±0.02	0.56±0.03	0.56±0.04	0.52±0.01	0.52±0.01	0.53±0.01	0.52±0.01	0.535±0.006
ours	<b>0.76±0.01</b>	<b>0.70±0.01</b>	<b>0.71±0.03</b>	<b>0.71±0.01</b>	<b>0.70±0.02</b>	<b>0.67±0.01</b>	<b>0.61±0.01</b>	<b>0.67±0.01</b>	<b>0.691±0.004</b>

Table 2: Classification accuracies for linear classifiers on top of learned representations and other supervised models. The train/test split is the same for all models.

Method	female	male	blond	darkhaired	smiles	nosmile	old	young	Mean
EEGNet	<b>0.76±0.01</b>	0.67±0.01	<b>0.74±0.02</b>	<b>0.71±0.03</b>	<b>0.72±0.01</b>	<b>0.69±0.01</b>	<b>0.64±0.02</b>	<b>0.68±0.01</b>	0.700±0.005
LDA	0.58±0.01	0.54±0.01	0.56±0.02	0.55±0.02	0.56±0.01	0.55±0.01	0.53±0.01	0.55±0.01	0.553±0.005
random control	0.52±0.02	0.53±0.02	0.53±0.01	0.52±0.02	0.51±0.01	0.51±0.01	0.51±0.01	0.54±0.01	0.519±0.004
ours	<b>0.76±0.01</b>	<b>0.70±0.02</b>	0.73±0.01	<b>0.71±0.01</b>	0.71±0.01	0.68±0.01	0.63±0.01	0.65±0.02	<b>0.701±0.005</b>

that the learned embeddings were effective in disentangling semantic features. Furthermore, we observed that the mean accuracy across all tasks is higher than that of the EEGNet, which suggests that the learned embeddings successfully reduced the high dimensionality of raw EEG signals while preserving the saliency perceived by the participant. It is worth noting that, the embedding model is trained without labels and the supervised linear classifier on top of it is expected to have relatively lower performance compared to a completely supervised model, as shown in [11].

#### 4.4 Personalized Model Evaluation

**Evaluation procedure.** To extend our model’s utility to accurately reflect individual cognitive responses, we evaluated fine-tuned personalized models. For each of the 30 participants, a base model was initially trained using EEG data from the other 29 participants. The target participant’s data was then divided into a 5-fold training set and a test set. We froze the base model’s weights, with the exception of the participant-specific matrix, which was randomly initialized and then fine-tuned using the single-participant training set. Frozen saliency embeddings from other participants were used to assist in selecting the target cluster.

**Control models.** For comparison, we also evaluated two control models. The first control model is the base model evaluated on the test set without fine-tuning. The target participant matrix is set to

the identity matrix. The second control model was fine-tuned on randomly shuffled training data, breaking the pairs of EEG signals and stimuli vectors.

**Results.** Table 3 presents the mean clustering accuracy on the test set and reports the mean from 5-fold validation across all participants. The personalized models demonstrated a small improved accuracy over the base models on average on all tasks. Our results suggest that with more data available, our method has the potential to further improve. In addition, the base model, which was not trained with personal data, still achieved a high clustering accuracy compared to the random control model. This underscores the zero-shot prediction capability of our embedding model, highlighting its potential to learn robust representations and adapt to the subjective information from individual cognitive signals.

#### 4.5 Qualitative evaluation via generative visualization

**Generative Visualization of Salient Features.** In order to provide an intuitive understanding of the inter-subject variations, we visualize the embeddings for a qualitative evaluation. We sample a set  $S$  of candidate stimuli vectors which can be the set of stimuli vectors in the training set, or a fresh set of randomly sampled vectors from the noise distribution used in the generative model.

**Table 3: Clustering accuracies of all personalized models.**

Model	female	male	blond	darkhaired	smiles	nosmile	old	young	Mean
random control	0.56±0.01	0.53±0.01	0.55±0.02	0.55±0.01	0.51±0.01	0.52±0.01	0.52±0.01	0.55±0.01	0.537±0.025
base model	<b>0.74±0.01</b>	0.66±0.01	<b>0.70±0.01</b>	<b>0.68±0.01</b>	<b>0.70±0.01</b>	0.65±0.01	0.61±0.01	0.65±0.01	0.673±0.020
personalized model	<b>0.74±0.01</b>	<b>0.67±0.01</b>	<b>0.70±0.01</b>	<b>0.68±0.01</b>	<b>0.70±0.01</b>	<b>0.66±0.01</b>	<b>0.62±0.01</b>	<b>0.66±0.01</b>	<b>0.682±0.021</b>

**Table 4: Clustering accuracies of model variants in ablation study.**

Model Variant	female	male	blond	darkhaired	smiles	nosmile	old	young	Mean
full model	<b>0.76±0.01</b>	<b>0.70±0.01</b>	<b>0.71±0.03</b>	<b>0.71±0.01</b>	<b>0.70±0.02</b>	<b>0.67±0.01</b>	0.61±0.01	<b>0.67±0.01</b>	<b>0.691±0.005</b>
$M_{\text{base}}$	0.75±0.02	0.64±0.01	0.68±0.01	0.67±0.02	0.66±0.01	0.64±0.05	0.60±0.02	0.64±0.01	0.660±0.007
$M_{\text{no augmentation}}$	0.75±0.01	0.66±0.02	0.69±0.01	0.69±0.01	0.67±0.02	0.62±0.01	0.54±0.08	0.64±0.02	0.658±0.011
$M_{\text{no matrix}}$	0.73±0.01	0.65±0.02	0.70±0.01	0.67±0.01	<b>0.70±0.01</b>	0.65±0.01	<b>0.62±0.01</b>	0.64±0.01	0.668±0.003

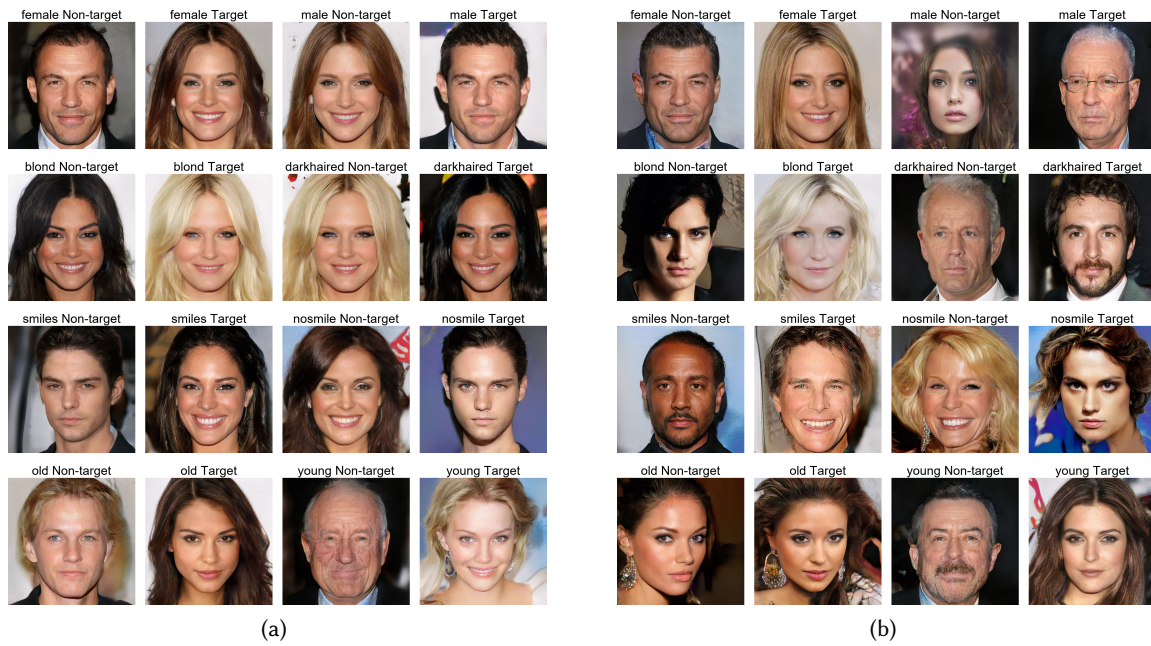


**Figure 4: Visualization of clusters by mapping to (a) stimuli vectors from the training set and (b) randomly sampled vectors not from the training set. Each of the eight tasks results in a Target cluster and a Non-target cluster. The visualization of Target cluster should match the task description (female, male, blond, dark hair, smiles, nosmile, old, young) and Non-target visualization should not.**

Each embedding  $Z$  in a cluster  $C$  is mapped to one of these stimuli  $v_Z = \operatorname{argmax}_{Y \in S} \langle Z, Y \rangle$ , and use the mean  $M_C = \frac{1}{|C|} \sum_{Z \in C} v_Z$  to represent the cluster. We visualize it using the pre-trained generative model. For each task, we expect the image generated from  $M_{C_{\text{Target}}}$  to contain salient task-specific semantic features and  $M_{C_{\text{Non-target}}}$  to have the opposite semantic saliency.

**Results.** The generated images with the stimuli set and the randomly sampled set are shown in Figure 4. Between the images

from  $M_{C_{\text{Target}}}$  and  $M_{C_{\text{Non-target}}}$ , it can be clearly seen that the semantic difference in images is correlated to the semantic task given to the participants. In Figure 4a the candidate image vectors are the stimuli vectors from the training set. In Figure 4b, 600 randomly sampled 512 vectors that are not present in the training set, are used as candidate sets and the semantic difference matching the task is still present. The salient features are clearly present across the different tasks and not present in the opposite tasks (Figure 4a).

The representations result in generated images in which the intended salient features are present even for randomly sampled candidates (Figure 4b). This indicates that the learned embeddings reflect the underlying signal from human cognition for generating task-specific salient features.

For each individual, we also visualized the subset of embeddings from a single participant similarly in supplementary materials Sec. A1.

#### 4.6 Ablation Analysis

An ablation study was conducted to study the effects of participant-specific matrices and data augmentation. In contrast to the full model, three variants of the models were trained: (a)  $M_{\text{no matrix}}$  that removes the participant-specific matrix; (b)  $M_{\text{no augmentation}}$  that removes data augmentation; (c)  $M_{\text{base}}$  that removes both.

The base model  $M_{\text{base}}$  and  $M_{\text{no matrix}}$  assumes that all data are collected from the same participant, and we select the cluster with the higher ERP effect as the target cluster. To minimize the differences caused by random cropping in data augmentation or other dimension changes, the base model  $M_{\text{base}}$  and  $M_{\text{no augmentation}}$  crops the EEG signals with fixed intervals as used in the test set.

Table 4 shows the accuracies of the full model and other variants for each task. The full model with the participant-specific matrix and augmentation consistently yields improved accuracy over all model variants in all tasks except the task old. The two variant models  $M_{\text{no matrix}}$  and  $M_{\text{no augmentation}}$  both have improved mean accuracy over the base model.

### 5 DISCUSSION

We presented cognitive supervision that allows to use EEG brain recordings and stimuli information to learn embeddings that capture differences in visual saliency without any external labels. Below, we reflect on the two research questions we posed.

**Can representations of semantic saliency be directly learned from EEG data as a supervision signal?** We introduced a novel approach for contrastive training of models supervised solely by brain signals, demonstrating the feasibility of learning semantic visual saliencies from EEG signals. Our models successfully capture semantic saliency without relying on explicit manual annotations.

**Do the learned representations accurately capture the salient features in downstream tasks?** We evaluated the performance of our models in classification, clustering, and image generation tasks using facial image data. The results indicate enhanced performance across these tasks, comparable to classification models pre-trained and fine-tuned with extensive labeled datasets. In image generation tasks, the models demonstrate capabilities that are both valid and competitive, even when compared to models trained with manually annotated data.

**Limitations.** Currently, the field of brain-computer interfacing, while advancing, is predominantly challenged by issues of accuracy and practical convenience when compared to established user interfaces. Our experimental setup, although innovative, is principally confined to the laboratory environment and may not yet translate seamlessly to widespread public use. Nevertheless, our experiments underscore the potential to cultivate human-in-the-loop learning

systems that directly engage with human cognitive processing. These systems do not depend on manual labeling, nor do they rely on the often inaccurate and indirect manual annotations or implicit behavioral indicators. A distinct limitation of our method lies in its focus on discerning between target or non-target saliency at an individual level, essentially capturing whether an item of visual information holds salience or not. This dichotomy means our technique is not apt for annotation tasks demanding explicit labels but rather suits recognition scenarios that model individual preferences or where the task itself delineates the saliency. Examples where our method could be particularly effective include enhancing image search accuracy, CAPTCHA image detection, or in contexts where a saliency detection task is predefined for participants. Despite these limitations, numerous outcomes from our research suggest that the capabilities of models trained under our cognitive supervision framework often exceed those of models trained via conventional manual labeling. This efficacy highlights the potential of leveraging cognitive supervision to substantially refine machine learning, offering a pathway to discern human preferences toward visually salient features in a completely passive manner.

### 6 CONCLUSIONS

We have pioneered a novel demonstration that machine learning systems can be self-supervised directly from human cognitive signals captured through EEG, to detect saliency of information perceived by the user. This approach paves the way for developing machine learning systems that incorporate human-in-the-loop interactions by real-time monitoring of cognitive reactions toward digital content. While this represents a powerful new paradigm in machine learning, capable of learning user reactions to information encountered and experienced in the digital world, it also surfaces significant ethical concerns. These arise not from the recording technology per se but from the potential for broader application of cognitive signal monitoring. As technological development progresses, demonstrating that models can learn autonomously from brain responses without the need for explicit task labels or calibration, there's an increasing risk associated with the pervasive collection and use of cognitive data. Such practices, if overlooked, could enable the inference of individual and collective attitudes towards a broad spectrum of digital content, as evidenced in our initial experiments.

Therefore, the use of data must be regulated with adequate policies that can prevent lasting threats to the public. To this end, there are already actions circumventing unethical use. For instance, the EU AI act<sup>3</sup> prevents AI systems for the purpose of identifying or inferring emotions or intentions of natural persons on the basis of their biometric data in the workplace and educational institutions.

However, the policies are only regulating specific use cases. With this work, we call for more academic investigation to understand what is possible, theoretically and empirically, with this novel technology to formulate robust guidelines ensuring the responsible adoption and use of cognitive supervision technologies.

<sup>3</sup><https://digital-strategy.ec.europa.eu/en/policies/regulatory-framework-ai>



## REFERENCES

- [1] Hamad Ahmed, Ronnie B Wilbur, Hari M Bharadwaj, and Jeffrey Mark Siskind. 2021. Confounds in the data—Comments on “Decoding brain representations by multimodal learning of neural activity and visual features”. *IEEE transactions on pattern analysis and machine intelligence* 44, 12 (2021), 9217–9220.
- [2] Hamad Ahmed, Ronnie B Wilbur, Hari M Bharadwaj, and Jeffrey Mark Siskind. 2021. Object classification from randomized EEG trials. In *Proceedings of the IEEE/CVF Conference on Computer Vision and Pattern Recognition*. 3845–3854.
- [3] Abeer Al-Nafjan, Manar Hosny, Yousef Al-Ohali, and Areej Al-Wabil. 2017. Review and classification of emotion recognition based on EEG brain-computer interface system research: a systematic review. *Applied Sciences* 7, 12 (2017), 1239.
- [4] P Aricò, G Borghini, G Di Flumeri, A Colosimo, S Pozzi, and F Babiloni. 2016. A passive brain-computer interface application for the mental workload assessment on professional air traffic controllers during realistic air traffic control tasks. *Progress in brain research* 228 (2016), 295–328.
- [5] Philip Bachman, R Devon Hjelm, and William Buchwalter. 2019. Learning representations by maximizing mutual information across views. *Advances in neural information processing systems* 32 (2019).
- [6] Hubert Banville, Omar Chehab, Aapo Hyvärinen, Denis-Alexander Engemann, and Alexandre Gramfort. 2021. Uncovering the structure of clinical EEG signals with self-supervised learning. *Journal of Neural Engineering* 18, 4 (2021), 046020.
- [7] Benjamin Blankertz, Steven Lemm, Matthias Treder, Stefan Haufe, and Klaus-Robert Müller. 2011. Single-trial analysis and classification of ERP components—a tutorial. *NeuroImage* 56, 2 (2011), 814–825.
- [8] Stanislas Chambon, Mathieu N Galtier, Pierrick J Arnal, Gilles Wainrib, and Alexandre Gramfort. 2018. A deep learning architecture for temporal sleep stage classification using multivariate and multimodal time series. *IEEE Transactions on Neural Systems and Rehabilitation Engineering* 26, 4 (2018), 758–769.
- [9] Tao Chen, Haiyun Huang, Jiahui Pan, and Yuanqing Li. 2018. An EEG-based brain-computer interface for automatic sleep stage classification. In *2018 13th IEEE Conference on Industrial Electronics and Applications (ICIEA)*. IEEE, 1988–1991.
- [10] Ting Chen, Simon Kornblith, Mohammad Norouzi, and Geoffrey Hinton. 2020. A simple framework for contrastive learning of visual representations. In *International conference on machine learning*. PMLR, 1597–1607.
- [11] Ting Chen, Simon Kornblith, Kevin Swersky, Mohammad Norouzi, and Geoffrey Hinton. 2020. Big Self-Supervised Models are Strong Semi-Supervised Learners. *arXiv preprint arXiv:2006.10029* (2020).
- [12] Ting Chen, Saurabh Saxena, Lala Li, David J Fleet, and Geoffrey Hinton. 2021. Pix2seq: A language modeling framework for object detection. *arXiv preprint arXiv:2109.10852* (2021).
- [13] Elijah Cole, Xuan Yang, Kimberly Wilber, Oisín Mac Aodha, and Serge Belongie. 2022. When does contrastive visual representation learning work? In *Proceedings of the IEEE/CVF Conference on Computer Vision and Pattern Recognition*. 14755–14764.
- [14] Ciaran Cooney, Raffaella Folli, and Damien Coyle. 2019. Optimizing Layers Improves CNN Generalization and Transfer Learning for Imagined Speech Decoding from EEG. In *2019 IEEE International Conference on Systems, Man and Cybernetics (SMC)*. 1311–1316. <https://doi.org/10.1109/SMC.2019.8914246>
- [15] Victor Guilherme Turrissi Da Costa, Enrico Fini, Moin Nabi, Nicu Sebe, and Elisa Ricci. 2022. solo-learn: A Library of Self-supervised Methods for Visual Representation Learning. *J. Mach. Learn. Res.* 23, 56 (2022), 1–6.
- [16] Joseph DelPreto, Andres F Salazar-Gomez, Stephanie Gil, Ramin Hasani, Frank H Guenther, and Daniela Rus. 2020. Plug-and-play supervisory control using muscle and brain signals for real-time gesture and error detection. *Autonomous Robots* 44 (2020), 1303–1322.
- [17] Alexandre Défossez, Charlotte Caucheteux, Jérémy Rapin, Ori Kabeli, and Jean-Rémi King. 2022. Decoding speech from non-invasive brain recordings. <https://doi.org/10.48550/ARXIV.2208.12266>
- [18] Nesma E. Elsayed, Ahmed S. Tolba, Magdi Z. Rashad, Tamer Belal, and Shahenda Sarhan. 2021. A Deep Learning Approach for Brain Computer Interaction-Motor Execution EEG Signal Classification. *IEEE Access* 9 (2021), 101513–101529. <https://doi.org/10.1109/ACCESS.2021.3097797>
- [19] Manuel JA Eugster, Tuukka Ruotsalo, Michael M Spapé, Ilkka Kosunen, Oswald Barral, Niklas Ravaja, Giulio Jacucci, and Samuel Kaski. 2014. Predicting term-relevance from brain signals. In *Proceedings of the 37th international ACM SIGIR conference on Research & development in information retrieval*. 425–434.
- [20] Beliz Gunel, Jingfei Du, Alexis Conneau, and Veselin Stoyanov. 2021. Supervised Contrastive Learning for Pre-trained Language Model Fine-tuning. In *International Conference on Learning Representations*.
- [21] Kaiming He, Xinlei Chen, Saining Xie, Yanghao Li, Piotr Dollár, and Ross Girshick. 2022. Masked autoencoders are scalable vision learners. In *Proceedings of the IEEE/CVF Conference on Computer Vision and Pattern Recognition*. 16000–16009.
- [22] Kaiming He, Haoqi Fan, Yuxin Wu, Saining Xie, and Ross Girshick. 2020. Momentum contrast for unsupervised visual representation learning. In *Proceedings of the IEEE/CVF conference on computer vision and pattern recognition*. 9729–9738.
- [23] Kaiming He, Xiangyu Zhang, Shaoqing Ren, and Jian Sun. 2016. Deep residual learning for image recognition. In *Proceedings of the IEEE conference on computer vision and pattern recognition*. 770–778.
- [24] Haiyun Huang, Qiuyou Xie, Jiahui Pan, Yanbin He, Zhenfu Wen, Ronghao Yu, and Yuanqing Li. 2019. An EEG-based brain computer interface for emotion recognition and its application in patients with disorder of consciousness. *IEEE Transactions on Affective Computing* 12, 4 (2019), 832–842.
- [25] Ashish Jaiswal, Ashwin Ramesh Babu, Mohammad Zaki Zadeh, Debapriya Banerjee, and Fillia Makedon. 2020. A survey on contrastive self-supervised learning. *Technologies* 9, 1 (2020), 2.
- [26] Xue Jiang, Jianhui Zhao, Bo Du, and Zhiyong Yuan. 2021. Self-supervised contrastive learning for EEG-based sleep staging. In *2021 International Joint Conference on Neural Networks (IJCNN)*. IEEE, 1–8.
- [27] Thorsten Joachims, Laura Granka, Bing Pan, Helene Hembrooke, and Geri Gay. 2005. Accurately Interpreting Clickthrough Data as Implicit Feedback. In *Proceedings of the 28th Annual International ACM SIGIR Conference on Research and Development in Information Retrieval (Salvador, Brazil) (SIGIR '05)*. Association for Computing Machinery, New York, NY, USA, 154–161. <https://doi.org/10.1145/1076034.1076063>
- [28] Tero Karras, Timo Aila, Samuli Laine, and Jaakko Lehtinen. 2018. Progressive Growing of GANs for Improved Quality, Stability, and Variation. [arXiv:1710.10196](https://arxiv.org/abs/1710.10196) [cs.NE]
- [29] Isaak Kavasidis, Simone Palazzo, Concetto Spampinato, Daniela Giordano, and Mubarak Shah. 2017. Brain2image: Converting brain signals into images. In *Proceedings of the 25th ACM international conference on Multimedia*. 1809–1817.
- [30] Nastaran Khaleghi, Tohid Yousefi Rezaii, Soosan Beheshti, Saeed Meshgini, Sobhan Sheykhiwand, and Sebelan Danishvar. 2022. Visual saliency and image reconstruction from EEG signals via an effective geometric deep network-based generative adversarial network. *Electronics* 11, 21 (2022), 3637.
- [31] Alexander Kolesnikov, Xiaohua Zhai, and Lucas Beyer. 2019. Revisiting self-supervised visual representation learning. In *Proceedings of the IEEE/CVF conference on computer vision and pattern recognition*. 1920–1929.
- [32] Satyam Kumar, Hussein Alawieh, Frigyes Samuel Racz, Rawan Fakhreddine, and José del R Millán. 2024. Transfer learning promotes acquisition of individual BCI skills. *PNAS nexus* 3, 2 (2024), pgae076.
- [33] Vernon J Lawhern, Amelia J Solon, Nicholas R Waytowich, Stephen M Gordon, Chou P Hung, and Brent J Lance. 2018. EEGNet: a compact convolutional neural network for EEG-based brain-computer interfaces. *Journal of neural engineering* 15, 5 (2018), 056013.
- [34] Ren Li, Jared S Johansen, Hamad Ahmed, Thomas V Ilyevsky, Ronnie B Wilbur, Hari M Bharadwaj, and Jeffrey Mark Siskind. 2020. The perils and pitfalls of block design for EEG classification experiments. *IEEE Transactions on Pattern Analysis and Machine Intelligence* 43, 1 (2020), 316–333.
- [35] Ziwei Liu, Ping Luo, Xiaogang Wang, and Xiaoou Tang. 2015. Deep Learning Face Attributes in the Wild. In *Proceedings of International Conference on Computer Vision (ICCV)*.
- [36] Steven J. Luck. 2014. Artifact Rejection and Correction. In *An introduction to the event-related potential technique* (2nd ed.). MIT Press, Cambridge, Massachusetts, 185–217.
- [37] Julian McAuley. in press. *Personalized Machine Learning*. Cambridge University Press.
- [38] Rahul Mishra, Krishan Sharma, RR Jha, and Arnab Bhavsar. 2023. NeuroGAN: image reconstruction from EEG signals via an attention-based GAN. *Neural Computing and Applications* 35, 12 (2023), 9181–9192.
- [39] Mostafa Neo Mohsenvand, Mohammad Rasool Izadi, and Pattie Maes. 2020. Contrastive representation learning for electroencephalogram classification. In *Machine Learning for Health*. PMLR, 238–253.
- [40] Takashi Nishimoto, Hiroshi Higashi, Hiroshi Morioka, and Shin Ishii. 2020. EEG-based personal identification method using unsupervised feature extraction and its robustness against intra-subject variability. *Journal of Neural Engineering* 17, 2 (mar 2020), 026007. <https://doi.org/10.1088/1741-2552/ab6d89>
- [41] Aaron van den Oord, Yazhe Li, and Oriol Vinyals. 2018. Representation learning with contrastive predictive coding. *arXiv preprint arXiv:1807.03748* (2018).
- [42] Simone Palazzo, Concetto Spampinato, Isaak Kavasidis, Daniela Giordano, Joseph Schmidt, and Mubarak Shah. 2020. Decoding brain representations by multimodal learning of neural activity and visual features. *IEEE Transactions on Pattern Analysis and Machine Intelligence* 43, 11 (2020), 3833–3849.
- [43] Simone Palazzo, Concetto Spampinato, Isaak Kavasidis, Daniela Giordano, and Mubarak Shah. 2017. Generative adversarial networks conditioned by brain signals. In *Proceedings of the IEEE international conference on computer vision*. 3410–3418.
- [44] André Susano Pinto, Alexander Kolesnikov, Yuge Shi, Lucas Beyer, and Xiaohua Zhai. 2023. Tuning computer vision models with task rewards. <https://doi.org/10.48550/ARXIV.2302.08242>
- [45] Alec Radford, Jong Wook Kim, Chris Hallacy, Aditya Ramesh, Gabriel Goh, Sandhini Agarwal, Girish Sastry, Amanda Askell, Pamela Mishkin, Jack Clark, et al. 2021. Learning transferable visual models from natural language supervision. In *International Conference on Machine Learning*. PMLR, 8748–8763.

929  
930  
931  
932  
933  
934  
935  
936  
937  
938  
939  
940  
941  
942  
943  
944  
945  
946  
947  
948  
949  
950  
951  
952  
953  
954  
955  
956  
957  
958  
959  
960  
961  
962  
963  
964  
965  
966  
967  
968  
969  
970  
971  
972  
973  
974  
975  
976  
977  
978  
979  
980  
981  
982  
983  
984  
985  
986987  
988  
989  
990  
991  
992  
993  
994  
995  
996  
997  
998  
999  
1000  
1001  
1002  
1003  
1004  
1005  
1006  
1007  
1008  
1009  
1010  
1011  
1012  
1013  
1014  
1015  
1016  
1017  
1018  
1019  
1020  
1021  
1022  
1023  
1024  
1025  
1026  
1027  
1028  
1029  
1030  
1031  
1032  
1033  
1034  
1035  
1036  
1037  
1038  
1039  
1040  
1041  
1042  
1043  
1044

- 1045 [46] A Riccio, F Leotta, L Bianchi, F Aloise, C Zickler, EJ Hoogerwerf, A Kübler,  
1046 D Mattia, and F Cincotti. 2011. Workload measurement in a communication  
1047 application operated through a P300-based brain-computer interface. *Journal of*  
1048 *neural engineering* 8, 2 (2011), 025028.
- 1049 [47] Aaqib Saeed, David Grangier, and Neil Zeghidour. 2021. Contrastive learning of  
1050 general-purpose audio representations. In *ICASSP 2021-2021 IEEE International*  
1051 *Conference on Acoustics, Speech and Signal Processing (ICASSP)*. IEEE, 3875–3879.
- 1052 [48] Eduardo Santamaría-Vázquez, Víctor Martínez-Cagigal, Fernando Vaquerizo-  
1053 Villar, and Roberto Hornero. 2020. EEG-Inception: A Novel Deep Convolutional  
1054 Neural Network for Assistive ERP-Based Brain-Computer Interfaces. *IEEE Trans-*  
1055 *actions on Neural Systems and Rehabilitation Engineering* 28, 12 (2020), 2773–2782.  
1056 <https://doi.org/10.1109/TNSRE.2020.3048106>
- 1057 [49] Steffen Schneider, Jin Hwa Lee, and Mackenzie Weygandt Mathis. 2023. Learnable  
1058 latent embeddings for joint behavioural and neural analysis. *Nature* (2023), 1–9.
- 1059 [50] Si Shen, Botao Hu, Weizhu Chen, and Qiang Yang. 2012. Personalized click model  
1060 through collaborative filtering. In *Proceedings of the fifth ACM international*  
1061 *conference on Web search and data mining*. 323–332.
- 1062 [51] Prajwal Singh, Pankaj Pandey, Krishna Miyapuram, and Shanmuganathan Raman.  
1063 2023. EEG2IMAGE: Image reconstruction from EEG brain signals. In *ICASSP*  
1064 *2023-2023 IEEE International Conference on Acoustics, Speech and Signal Processing*  
1065 *(ICASSP)*. IEEE, 1–5.
- 1066 [52] Concetto Spampinato, Simone Palazzo, Isaak Kavasidis, Daniela Giordano, Nasim  
1067 Souly, and Mubarak Shah. 2017. Deep learning human mind for automated visual  
1068 classification. In *Proceedings of the IEEE conference on computer vision and pattern*  
1069 *recognition*. 6809–6817.
- 1070 [53] Yu Takagi and Shinji Nishimoto. 2022. High-resolution image reconstruction  
1071 with latent diffusion models from human brain activity. *bioRxiv* (2022), 2022–11.
- 1072 [54] Praveen Tirupattur, Yogesh Singh Rawat, Concetto Spampinato, and Mubarak  
1073 Shah. 2018. Thoughtviz: Visualizing human thoughts using generative adversarial  
1074 network. In *Proceedings of the 26th ACM international conference on Multimedia*.  
1075 950–958.
- 1076 [55] Patrik Vuilleumier, Jorge L Armony, Jon Driver, and Raymond J Dolan. 2001. Effects of attention and emotion on face processing in the human brain: an event-related fMRI study. *Neuron* 30, 3 (2001), 829–841.
- 1077 [56] Xiao Wang and Guo-Jun Qi. 2022. Contrastive learning with stronger augmentations. *IEEE Transactions on Pattern Analysis and Machine Intelligence* (2022).
- 1078 [57] Haohang Xu, Xiaopeng Zhang, Hao Li, Lingxi Xie, Wenrui Dai, Hongkai Xiong, and Qi Tian. 2022. Seed the views: Hierarchical semantic alignment for contrastive representation learning. *IEEE Transactions on Pattern Analysis and Machine Intelligence* (2022).
- 1079 [58] Liangwei Yang, Zhiwei Liu, Yu Wang, Chen Wang, Ziwei Fan, and Philip S Yu. 2022. Large-scale personalized video game recommendation via social-aware contextualized graph neural network. In *Proceedings of the ACM Web Conference 2022*. 3376–3386.
- 1080 [59] Xing Yi, Liangjie Hong, Erheng Zhong, Nanthan Nan Liu, and Suju Rajan. 2014. Beyond clicks: dwell time for personalization. In *Proceedings of the 8th ACM Conference on Recommender systems*. 113–120.
- 1081 [60] Xin Yuan, Zhe Lin, Jason Kuen, Jianming Zhang, Yilin Wang, Michael Maire, Ajinkya Kale, and Baldo Faieta. 2021. Multimodal contrastive training for visual representation learning. In *Proceedings of the IEEE/CVF Conference on Computer Vision and Pattern Recognition*. 6995–7004.
- 1082 [61] Hong Zeng, Nianzhang Xia, Dongguan Qian, Motonobu Hattori, Chu Wang, and Wanzeng Kong. 2023. DM-RE2I: A framework based on diffusion model for the reconstruction from EEG to image. *Biomedical Signal Processing and Control* 86 (2023), 105125.
- 1083 [62] Xiao Zheng, Wanzhong Chen, Yang You, Yun Jiang, Mingyang Li, and Tao Zhang. 2020. Ensemble deep learning for automated visual classification using EEG signals. *Pattern Recognition* 102 (2020), 107147. <https://doi.org/10.1016/j.patcog.2019.107147>
- 1084 [63] Qiongyi Zhou, Changde Du, Shengpei Wang, and Huiguang He. 2024. CLIP-MUSED: CLIP-Guided Multi-Subject Visual Neural Information Semantic Decoding. *arXiv preprint arXiv:2402.08994* (2024).
- 1085 1103
- 1086 1104
- 1087 1105
- 1088 1106
- 1089 1107
- 1090 1108
- 1091 1109
- 1092 1110
- 1093 1111
- 1094 1112
- 1095 1113
- 1096 1114
- 1097 1115
- 1098 1116
- 1099 1117
- 1100 1118
- 1101 1119
- 1102 1120
- 1121
- 1122
- 1123
- 1124
- 1125
- 1126
- 1127
- 1128
- 1129
- 1130
- 1131
- 1132
- 1133
- 1134
- 1135
- 1136
- 1137
- 1138
- 1139
- 1140
- 1141
- 1142
- 1143
- 1144
- 1145
- 1146
- 1147
- 1148
- 1149
- 1150
- 1151
- 1152
- 1153
- 1154
- 1155
- 1156
- 1157
- 1158
- 1159
- 1160